Polymers of Intrinsic Microporosity Derived from Bis(phenazyl) Monomers

Bader S. Ghanem,[†] Neil B. McKeown,*[,†] Peter M. Budd,[‡] and Detlev Fritsch[§]

School of Chemistry, Cardiff University, Cardiff, CF10 3AT, U.K., Organic Materials Innovation Centre, School of Chemistry, University of Manchester, Manchester, M13 9PL, U.K., and Institute of Polymer Research, GKSS Research Centre Geesthacht GmbH, Max-Planck-Strasse 1, D-21502 Geesthacht, Germany

Received August 15, 2007; Revised Manuscript Received December 11, 2007

ABSTRACT: Novel polymers of intrinsic microporosity (PIMs) are prepared from bis(phenazyl) monomers derived from readily available bis(catechol)s. One of the polymers (termed **PIM-7**) has an excellent combination of properties with high internal surface area, good film-forming characteristics, and gas transport properties that make it a suitable candidate for gas separation membranes. The high gas permeability and good ideal selectivity of **PIM-7** place it above Robeson's upper-bound for a number of commercially important gas pairs (e.g., O_2/N_2, CO_2/CH_4, and CO_2/N_2).

Introduction

Microporous materials, such as zeolites or activated carbons, contain interconnected molecular-sized pores (<2 nm) and are of great value as heterogeneous catalysts and adsorbents. Most polymers do not form solids that display classical microporosity because their conformational mobility allows the constituent macromolecules to fill space efficiently. However, microporous polymer-based materials can be obtained by the extensive crosslinking of solvent swollen polymers (e.g., hypercrosslinked polystyrenes)[1,2] or by preparing polymer networks using rigid monomers.[3−10] In addition, certain highly rigid, non-network polymers, for example poly(trimethylsilylpropyne),[11,12] certain polyimides,[13] and a number of fluorinated polymers,[14] form solids with very large free volumes so that they too can behave as microporous materials. These high-free volume polymers are soluble and, therefore, can be processed into forms that are useful as membranes for gas separations and water purification. Recently, we have described a novel class of high-free volume polymer termed polymers of intrinsic microporosity (PIMs) that are composed of rigid and contorted macromolecules, wholly composed of fused-rings some of which are spirocyclic.[15−19] PIMs form microporous organic materials due to their inability to pack space efficiently. PIMs combine high internal surface areas with the synthetic diversity of step-growth polymers and can be used for a wide range of applications including heterogeneous catalysis,[10,19] membrane separations,[15,20] hydrogen storage,[6,7,21,22] and the adsorption of organic compounds.[10,23]

The archetypal PIM, termed **PIM-1** (Scheme 1), is prepared as a high molecular mass, soluble polymer from the dioxane-forming reaction between commercially available 5,5′,6,6′-tetrahydroxy-3,3,3′,3′-tetramethyl-1,1′-spirobisindane (monomer **1**) and 2,3,5,6-tetrafluoroterephthalonitrile, which is an efficient double aromatic nucleophilic substitution reaction (S_NAr).[15,16] The spiro-center (i.e., a single tetrahedral carbon atom shared by two rings) of monomer **1** provides the site of contortion necessary for solubility and microporosity. On reprecipitation, **PIM-1** provides microporous powder with a surface area of 780 $m^2\ g^{-1}$ and can be cast from solution into robust free-standing films that show great promise for gas separations.[20] A number of other bis(catechol) monomers have also been used for PIM synthesis (**PIMs-2−6**)[16] but there are no readily available tetrahalide monomers that contain spiro-centers to provide a suitable site of contortion. This paper describes the simple synthesis of suitably reactive tetrachloride monomers **4** and **5** based on phenazine units prepared directly from suitable bis-(catechol) monomers such as **1** and 2,3,6,7-tetrahydroxy-9,10-dimethyl-9,10-ethanoanthracene **2**. The properties and potential applications of the PIMs (**PIMs-7−10**) derived from these novel monomers are discussed (Scheme 2). In addition, the properties of two novel "cardo" polymers (**Cardo-PIMs 1** and **2**) derived from the phenazyl monomers and 9,9-bis(3,4-hydroxyphenyl)-fluorene **3** are compared to the PIMs that contain fully fused-ring structures.

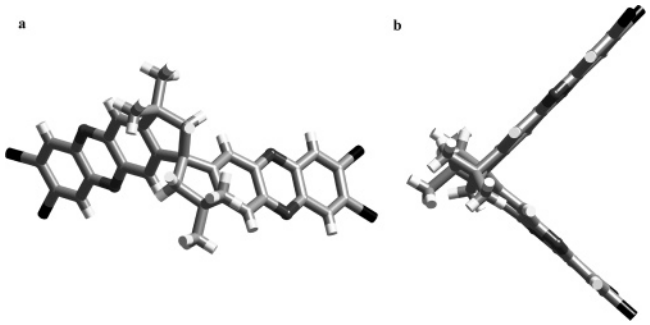

Figure 1. The structure of monomer **4** (a) face on and (b) in the plane, as determined from a single-crystal X-ray diffraction study showing the site of contortion provided by the spiro-center. (Raftery, J.; Ghanem, B. S.; McKeown, N. B. Report in preparation).

Experimental Section

Materials and Methods. All materials including monomer **1** (5,5′,6,6′-tetrahydroxy-3,3,3′,3′-tetramethyl-1,1′-spirobisindane) were obtained from Aldrich Chemical Co. or Lancaster Synthesis Ltd. and were used without purification. Monomer **2** (2,3,6,7-tetrahydroxy-9,10-dimethyl-9,10-ethanoanthracene) was prepared from catechol and 2,5-hexanedione following a literature procedure.[24−26] Monomer **3** (9,9-bis(3,4-dihydroxyphenyl)fluorene) was prepared

* To whom correspondence should be addressed. Prof. Neil B. McKeown, E-mail, mckeownnb@cardiff.ac.uk; Phone, +44 (0)2920-875851, School of Chemistry, Cardiff University, Cardiff, CF10 3AT, U.K.
† Cardiff University.
‡ University of Manchester.
§ GKSS Research Centre Geesthacht GmbH.

10.1021/ma071846r CCC: $40.75
Published on Web 02/12/2008

Scheme 1. The Synthesis and Structure of PIM-1[a]

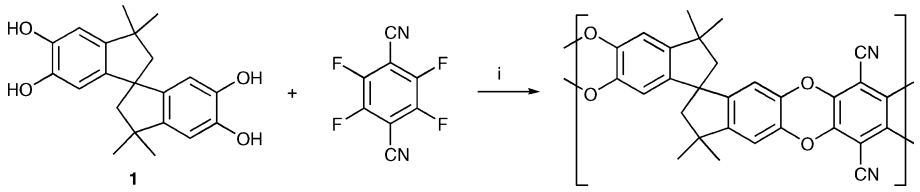

[a] Reagent and conditions: K_2CO_3, DMF, 65 °C, 48 h.

by the reaction of veratrol and fluorenone followed by demethylation using BBr_3, which is a minor adaptation of a literature procedure.[27] Silica gel (60 Merck 9385) was used in the separation and purification of compounds by column chromatography. All materials were heated at 120−150 °C under vacuum for 18 h as the final step of purification. Analytical HPLC analyses were performed using a phenosphere silica 5u column (4.6 mm × 250 mm) in 4:1 hexane/ethyl acetate V/V at a flow rate of 1.0 mL/min with a Perkin-Elmer LC-480 diode array detector at 255 nm. Elemental analyses were obtained using a Carlo Erba Instruments CHNS-O EA 108 elemental analyzer. The amount of chlorine was determined by potentiometric titration with a Metrohm auto titration system. Routine ^{1}H nuclear magnetic resonance (NMR) spectra were recorded using a Varian INOVA 300 MHz spectrometer, and high-resolution data (500 MHz) were recorded using a Varian Unity 500 spectrometer. IR spectra were recorded on an ATI Mattson Genesis series FTIR (KBr/Germanium beam splitter). Routine EI and CI mass spectra were recorded on a Fisons VG Trio 2000 instrument. MALDI mass spectra were recorded on a Micromass TOF Spec 2E instrument using a dithranol matrix doped with NaBr. Gel permeation chromatography (GPC) analysis was carried out using a set of Polymer Laboratories PLgel columns (two mixed-B and one 500 Å 10 μm) in $CHCl_3$ with Gilson 132 DR and Gilson 307 detectors using a Knauer 64 pump operating at a flow rate of 1 cm^3/min. Calibration was achieved using a series of polystyrene standards up to $M_w = 1.1 \times 10^6$ g mol^{-1}. Differential scanning calorimetry (DSC) measurements were made on a Seiko DSC 220C machine and calibrated using an indium standard. Thermogravimetric analysis (TGA) measurements were obtained using a Mettler FP82HT at a heating rate of 10 °C/min from room temperature to 600 °C. Low-temperature (77 K) N_2 adsorption/desorption measurements of PIM powders were made using a Coulter SA3100 (**PIMs-8−10** and **Cardo-PIMs-1** and **2**) or a Micromeritics ASAP 2020 analyzer (**PIM-7**). Samples were degassed for 2 days at 70 °C under high vacuum prior to analysis.

Bisquinone of 1. The monomer 5,5′6,6′-tetrahydroxy-3,3,3′3′-tetramethyl-1,1′-spirobisindane **(1)** (15 g, 44 mmol) was dissolved in hot ethanol (150 mL) and filtered. To the solution, a mixture of concentrated nitric acid (10 mL; *d* 1.42) and glacial acetic acid (10 mL) was added slowly while the temperature was kept at 0−5 °C. The mixture was kept at 0 °C for several hours and at room temperature for 24 h. The tetrone was then collected by filtration and washed with ethanol and water. The deep red product was boiled with water for 15 min and recrystallized twice from glacial acetic acid, washed with boiling water, and dried at 100 °C in a vacuum oven over sodium hydroxide (10.5 g, 74% yield); mp > 300 °C (found: C, 73.54; H, 6.08. Calculated for $C_{21}H_{20}O_4$: C, 74.9; H, 5.99.); δH (300 MHz, $CDCl_3$) 1.41 (s, 6H), 1.43 (s, 6H, CH_3), 2.26 (d, J = 13 Hz, 2H), 2.40 (d, J = 13 Hz, 2H), 6.19 (d, J = 1 Hz, 2H), 6.29 (d, J = 1 Hz, 2H); *m*/*z* (CI) 356 ($M^+ + NH_4$).

With the use of a similar procedure, the bisquinone was prepared from monomer 2,3,6,7-tetrahydroxy-9,10-dimethyl-9,10-ethanoanthracene **(2)** and recrystallized twice from chloroform/hexane to give a dark green powder (16 g, 81% yield), mp > 300 °C (found: C, 72.85; H, 4.69. Calculated for $C_{18}H_{14}O_4$: C, 73.46; H, 4.79.); δH (300 MHz, $CDCl_3$) 1.55 (s, 6H, CH_3), 2.06 (s, 4H), 6.29 (s, 4H); *m*/*z* (CI) 312 ($M^+ + NH_4$).

Monomer 4. To a stirred solution of 4,5-dichlorobenzene-1,2-diamine (2.10 g, 11.9 mmol) in glacial acetic acid (100 mL) was added the bisquinone of monomer **1** (1.0 g, 2.99 mmol). The reaction mixture was heated under reflux for 3 h under a nitrogen atmosphere. On cooling, the solid was collected by filtration and washed with acetic acid, water, and ethanol. Two recrystallizations from toluene gave the product as yellow crystals (1.3 g, 71% yield); mp > 300 °C (found: C, 64.85; H, 3.99; N, 8.87; Cl, 22.58. Calculated for $C_{33}H_{24}N_4Cl_4$: C, 64.1; H, 3.91; N, 9.06; Cl, 22.93.); δH ($CDCl_3$, 300 MHz) 1.62 (s, 6H, CH_3), 1.70 (s, 6H, CH_3), 2.69 (d, 2H, J = 13 Hz), 2.75 (d, 2H, J = 13 Hz, CH_2), 7.67 (s, 2H), 8.07 (s, 2H), 8.22 (s, 2H), 8.37 (s, 2H); IR (thin film cm^{-1}): ν =1098, 1353, 1420, 1590, 1635, 2851−2958, 3064; *m*/*z* (MALDI): 619 (M^+). The structure of 4 is shown in Figure 1.

With the use of a similar procedure, monomer **5** was prepared from the bisquinone of monomer **2** (4.9 g, 72% yield); mp > 300 °C (found: C, 61.88; H, 3.06; N, 9.65; Cl, 24.51. Calculated for $C_{30}H_{18}N_4Cl_4$: C, 62.52; H, 3.15; N, 9.72; Cl, 24.60.); δH ($CDCl_3$, 300 MHz) 2.06 (s, 4H), 2.33 (s, 6H), 8.17 (s, 4H), 8.39 (s, 4H). IR (KBr disk cm^{-1}): ν = 1098, 1417, 1602, 1639, 2857−2958, 3067; *m*/*z* (MALDI): 577 (M^+).

Model Compound 6. To a solution of catechol (0.215 g, 1.95 mmol) and monomer **4** (0.6 g, 0.97 mmol) in anhydrous DMF (50 mL) was added fine powdered anhydrous potassium carbonate (1.0 g, 7.25 mmol). The mixture was heated to 150 °C under a nitrogen atmosphere for 20 h, although monitoring of the reaction by MALDI-MS showed that the reaction was essentially complete after only 6 h. On cooling, the reaction mixture was added to distilled water (300 mL), and the crude product was collected by filtration, washed with copious amounts of distilled water, and recrystallized from chloroform/methanol to afford an orange powder (0.6 g, 88% yield); mp > 300 °C (found: C, 77.74; H, 4.34; N, 7.98. Calculated for $C_{45}H_{32}N_4O_4$: C, 78.02; H, 4.66; N, 8.09.); δH ($CDCl_3$, 300 MHz) 1.60 (s, 6H), 1.68 (s, 6H), 2.66 (d, 2H, J = 13 Hz, CH_2), 2.71 (d, 2H, J = 13 Hz), 7.03−7.06 (8H, m), 7.47 (s, 2H), 7.59 (s, 2H), 7.61 (s, 2H), 7.99 (s, 2H). IR (thin film cm^{-1}): ν = 1268, 1172, 1321, 1469, 1565, 1611, 2853−2955, 3111; *m*/*z* (MALDI) 693 (M^+); BET surface area = 4.2 m^2 g^{-1}.

PIM-7. To a stirred solution of monomer **1** (0.495 g, 1.455 mmol), monomer **4** (0.9 g, 1.455 mmol) and 18-crown-6 (0.385 g, 1.455 mmol) in anhydrous DMF (40 mL) was added anhydrous potassium carbonate (1.2 g, 8.7 mmol) and heating continued at 150 °C for 48 h. On cooling, the reaction mixture was poured into stirred aqueous HCl (1%, 500 mL), and the yellow-orange powder was collected by filtration, washed with distilled water and methanol, and then dried. A solution of the crude polymer in chloroform was filtered through glass wool and then reprecipitated by dropwise addition into THF. This procedure was repeated twice. The polymer was collected by filtration, dried in vacuum oven at 90 °C, and ground to give a yellow-orange powder (0.90 g, 76%) (found: C, 77.65; H, 5.42; N, 6.69; Cl, < 0.3. Calculated for $C_{54}H_{44}N_4O_4$ (repeat unit): C, 79.78; H, 5.46; N, 6.89.); δH ($CDCl_3$, 500 MHz) 1.22−1.63 (br m, 12H), 2.18−2.64 (br m, 8H), 6.51 (br s, 2H), 6.84 (br s, 2H), 7.34−7.56 (br m, 6H), 7.95 (br s, 2H). IR (thin film cm^{-1}): ν = 1168, 1220, 1327, 1467, 1609, 2864−2956, 3060−3100. Analysis by GPC ($CHCl_3$): M_n = 26 000, M_w = 51 000 g mol^{-1} relative to polystyrene. BET surface area = 680 m^2 g^{-1}, total pore volume = 0.56 cm^3 g^{-1} at (P/P_o = 0.98, adsorption). TGA analysis (nitrogen): 5% loss of weight occurred at 390 °C. Initial weight loss due to thermal degradation commences at ~410 °C. The THF soluble fraction was also a yellow-orange powder (0.20 g, 22% yield). Analysis by GPC (THF): M_n = 3950, M_w = 7200; surface area (BET) = 637 m^2 g^{-1}.

Scheme 2. The Synthesis of Monomers 4 and 5, Model Compound 6, and PIMs-7−10[a]

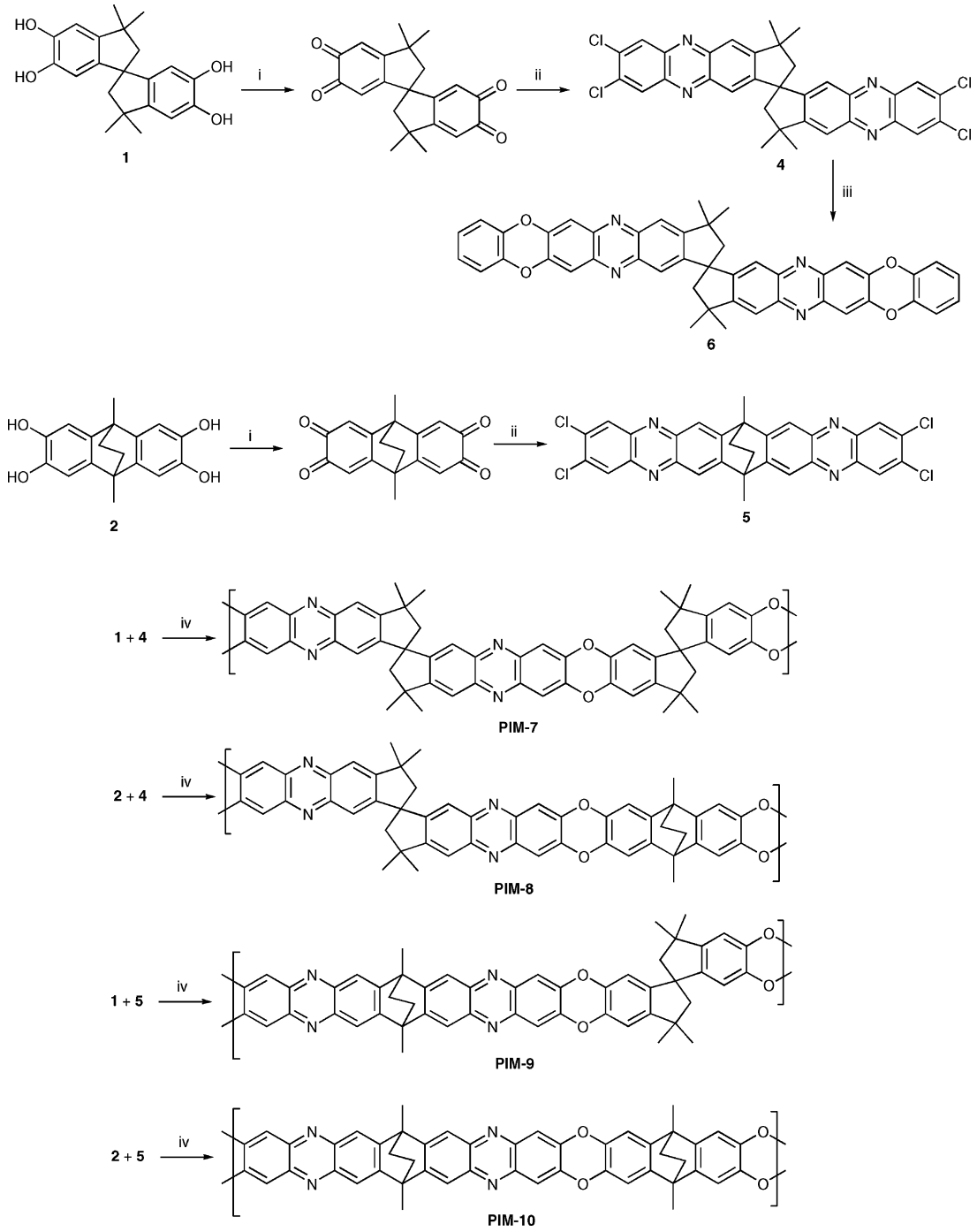

[a] Reagent and conditions: (i) nitric acid, AcOH, EtOH, 0 °C, 24 h; (ii) 1,2-diamino-4,5-dichlorobenzene, AcOH, reflux, 3 h; (iii) catechol, K_2CO_3, DMF, 150 °C, 20 h; (iv) K_2CO_3, 18-crown-6, DMF, 150 °C, 48 h.

The following polymers were prepared using the same procedure.

PIM-8. Monomer **2** (0.506 g, 1.697 mmol) and monomer **4** (1.05 g, 1.697 mmol) gave a yellow-orange powder (0.74 g; 71% after reprecipitation) (found: C, 76.63; H, 4.90; N, 7.08; Cl, 0.84. Calculated for $C_{51}H_{38}N_4O_4$ (repeat unit): C, 79.46; H, 4.97; N, 7.27.); δH ($CDCl_3$, 400 MHz) 1.45−1.86 (br m, 22H), 2.65 (br s, 4H), 6.95 (br s, 4H), 7.39 (br s, 2H), 7.53 (br s, 2H), 7.94 (br s, 2H). IR (thin film cm^{-1}): ν = 1168, 1240, 1269, 1325, 1454, 1607, 2864−2959, 3014−3068. Analysis by GPC ($CHCl_3$): M_n = 14 000, M_w = 406 100. BET surface area = 677 $m^2\ g^{-1}$, total pore volume = 0.48 $cm^3\ g^{-1}$ at (P/P_o = 0.98, adsorption). TGA analysis (nitrogen): 5% loss of weight occurred in the range of 385 °C. Initial weight loss due to thermal degradation commences at ~440 °C. The THF soluble fraction was also a yellow-orange powder (0.22 g, 21% yield). Analysis by GPC (THF) gave M_n = 2700, M_w = 3300. Surface area (BET) = 611 $m^2\ g^{-1}$.

PIM-9. Monomers **1** (0.60 g, 1.763 mmol) and monomer **5** (1.016 g, 1.763 mmol) gave a deep orange powder (1.06 g, 78% yield after reprecipitation) (found: C, 81.47; H, 5.81; N, 7.41. Calculated for $C_{51}H_{38}N_4O_4$ (repeat unit): C, 79.46; H, 4.97; N, 7.27.); δH ($CDCl_3$, 400 MHz) 1.30−1.65 (br m, 22H), 1.94−2.36 (br m, 4H), 6.54 (br s, 2H), 6.88 (br s, 2H), 7.41−7.55 (br m, 4H), 8.0 (br s, 4H); IR (thin film cm^{-1}): ν = 1172, 1220, 1324, 1465, 1609, 2863−2953, 3071. Analysis by GPC ($CHCl_3$): M_n = 13 000, M_w = 230 000. BET surface area = 661 $m^2\ g^{-1}$, total pore volume = 0.47 $cm^3\ g^{-1}$ at (P/P_o = 0.90, adsorption). TGA analysis (nitrogen): 5% loss of weight occurred in the range of 380 °C. Initial weight loss due to thermal degradation commences at

Scheme 3. The Synthesis of Cardo-PIMs-1 and 2[a]

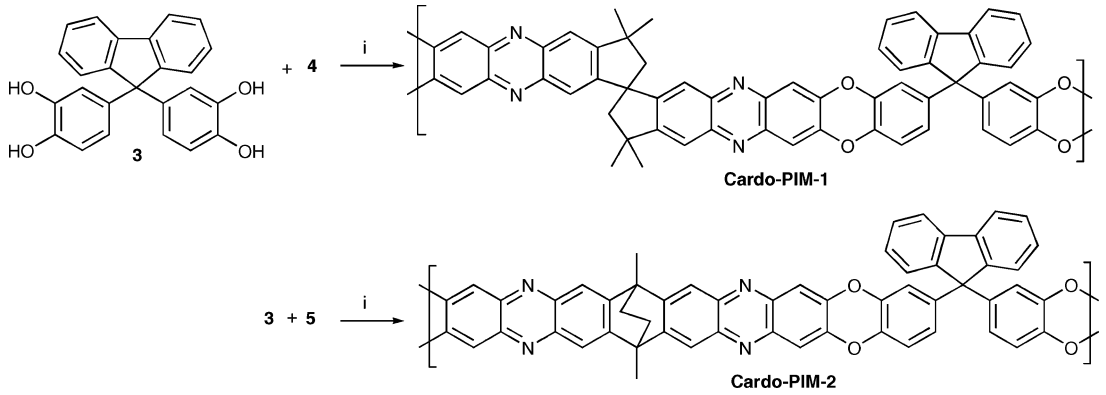

[a] Reagent and conditions: K_2CO_3, DMF, 150 °C, 48 h.

~400 °C. Analysis by GPC (THF) of the THF soluble fraction (0.30 g; 14%) gave $M_n = 1800$, $M_w = 2300$.

PIM-10. Monomer **2** (0.50 g, 1.676 mmol) and monomer **5** (0.966 g, 1.676 mmol) gave a deep orange powder the bulk of which proved insoluble in organic solvents (1.2 g, 98%) (found: C, 74.87; H, 4.53; N, 7.46; Cl, 1.5. Calculated for $C_{48}H_{32}N_4O_4$ (repeat unit): C, 79.1; H, 4.43; N, 7.68.); IR (KBr disk cm^{-1}): $\nu = 1168$, 1240, 1321, 1455, 1611, 2857−2958, 3068, 3450. BET surface area = 713 $m^2\ g^{-1}$, total pore volume = 0.44 $cm^3\ g^{-1}$ at ($P/P_o = 0.99$, adsorption). TGA analysis (nitrogen): 5% loss of weight occurred at ~340 °C. Initial weight loss due to thermal degradation commences at ~400 °C. GPC ($CHCl_3$) analysis for the chloroform soluble fraction (12 mg, 1%) gave $M_n = 3800$, $M_w = 5300$.

Cardo-PIM-1. Monomer **3** (0.618 g, 1.62 mmol) and monomer **4** (1.000 g, 1.62 mmol) gave a deep orange powder (1.15 g, 83% after reprecipitation) (found: C, 79.36; H, 4.58; N, 6.65; Cl, 0.63. Calculated for $C_{58}H_{38}N_4O_4$ (repeat unit): C, 81.48; H, 4.48; N, 6.55.); δH ($CDCl_3$, 400 MHz) 1.30−1.65 (br m, 12H), 2.63 (br m, 4H), 6.88 (br s, 6H), 7.33−7.53 (br m, 12H), 7.77 (br s, 2H), 7.93 (br s, 4H); IR (KBr disk cm^{-1}): $\nu = 1171$, 1240, 1320, 1466, 1605, 2857−2958, 3450. GPC ($CHCl_3$) analysis: $M_n = 30\,300$, $M_w = 867\,000$. BET surface area = 621 $m^2\ g^{-1}$; total pore volume = 0.51 $cm^3\ g^{-1}$ at ($P/P_o = 0.98$, adsorption). TGA analysis (nitrogen): 5% loss of weight occurred at ~480 °C. Initial weight loss due to thermal degradation commences at ~420 °C. GPC ($CHCl_3$) analysis for the chloroform soluble fraction (0.14 g; 10%) gave $M_n = 3600$, $M_w = 5260$.

Cardo-PIM-2. Monomer **3** (0.664 g, 1.74 mmol) and monomer **5** (1.000 g, 1.74 mmol) gave a deep orange powder the bulk of which proved insoluble in organic solvents (1.18 g, 84%) (found: C, 78.33; H, 4.24; N, 6.67; Cl, 0.40. Calculated for $C_{55}H_{32}N_4O_4$ (repeat unit): C, 81.27; H, 3.97; N, 6.89.); IR (KBr disk cm^{-1}): $\nu = 1171$, 1238, 1322, 1463, 1602, 2857−2955, 3062, 3450. BET surface area = 580 $m^2\ g^{-1}$; total pore volume = 0.63 $cm^3\ g^{-1}$ at ($P/P_o = 0.98$, adsorption). TGA analysis (nitrogen): 5% loss of weight occurred at ~385 °C. Initial weight loss due to thermal degradation commences at ~350 °C. GPC ($CHCl_3$) analysis for the chloroform soluble fraction (0.14 g; 10%) gave $M_n = 4700$, $M_w = 11\,200$.

Permeability Measurements. Films of **PIM-7** and **Cardo-PIM-1** of 28 and 27 μm thickness, respectively, were prepared by casting from a chloroform solution (2−5 wt %) into a flat-bottomed glass dish and allowing the solvent to evaporate slowly under a slow flow of N_2 at ambient temperature. Gas permeation data were measured at 30 °C with pure gases, using a pressure increase time-lag apparatus operated at low feed pressure (typically 200−300 mbar), starting with an oil free vacuum ($<10^{-4}$ mbar). Permeability coefficient, P, was calculated from the slope in the steady-state region and apparent diffusion coefficient, D, from the time-lag, θ, using $D = l^2/6\theta$, where l is the membrane thickness.

Results and Discussion

Synthesis. The phenazyl-based monomers **4** and **5** can be prepared in two steps from bis(catechol) monomers **1** and **2**, respectively (Scheme 2). Oxidation of the biscatechol with nitric acid,[28] or more efficiently with CAN,[29] produces the bisquinone which reacts with 1,2-diamino-4,5-dichlorobenzene in good yield (71%) to provide the monomers. The reactivity of the monomers toward dioxane formation was assessed by the ready synthesis of the model compound **6** from the reaction of catechol with monomer **4**. **PIMs-7−10** are prepared by the reactions between monomers **1** and **4**, **2** and **4**, **1** and **5**, and **2** and **5**, respectively. **PIMs-7−9** are soluble in a range of organic solvents (especially $CHCl_3$), but **PIM-10** is soluble only in *m*-cresol and concentrated H_2SO_4. Although self-supporting films could be cast from **PIMs-7−9**, the films from **PIM-7** were particularly flexible and robust. Therefore, the conditions for polymerization were optimized for this polymer (total monomer concentration of ~100 mmol/L in DMF at 150 °C for 48 h). Reactions with higher concentrations of monomer or temperatures produce insoluble polymer, presumably due to cross-linking whereas lower concentrations or temperatures tend to produce polymers of only moderate molecular mass. The addition of a small amount of 18-crown-6 is beneficial to attaining **PIM-7** of sufficient molecular mass for robust film formation.

So-called cardo-polymers contain cyclic units (e.g., fluorene) in which one of the carbon atoms in the ring is part of the polymer backbone and is related to spiropolymers within which a single atom within the backbone is shared by two rings. Such polymers have been shown to possess good characteristics for making gas separation membranes.[30−36] For a direct comparison with PIMs containing wholly fused ring structures, **Cardo-PIMs-1** and **2** were prepared by the reaction between 9,9-bis-(3,4-hydroxyphenyl)fluorene **3** and monomers **4** and **5**, respectively (Scheme 3). **Cardo-PIM-1** proved soluble in common organic solvent (e.g., $CHCl_3$) and possesses good film forming properties whereas **Cardo-PIM-2** is soluble only in cresol and concentrated H_2SO_4.

Structural Characterization. GPC confirmed that the polymers possess reasonably high average molecular mass. For example, purified **PIM-7** prepared under optimized reaction conditions has apparent average molecular masses of $M_n = 26\,000$ and $M_w = 51\,000$ g mol^{-1} relative to polystyrene standards. ^{1}H NMR spectra of **PIMs-7−9** and **Cardo-PIM-1** are consistent with their anticipated structures, however, there are no significant peaks that can be assigned to unreacted hydroxyl or dichlorinated phenazyl end-groups. Elemental

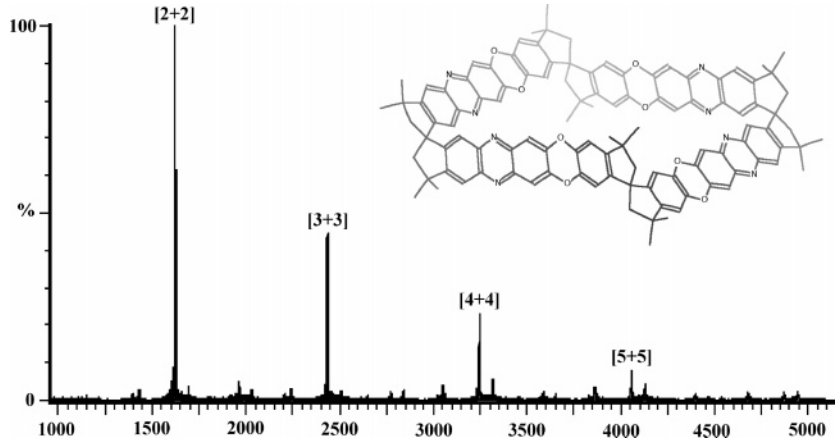

Figure 2. The MALDI-MS spectrum of the low molar mass fraction of **PIM-7** (i.e., THF soluble). The prominent peaks all correspond to the mass of cyclic oligomers, with the structure of the [2 + 2] oligomer shown in the inset.

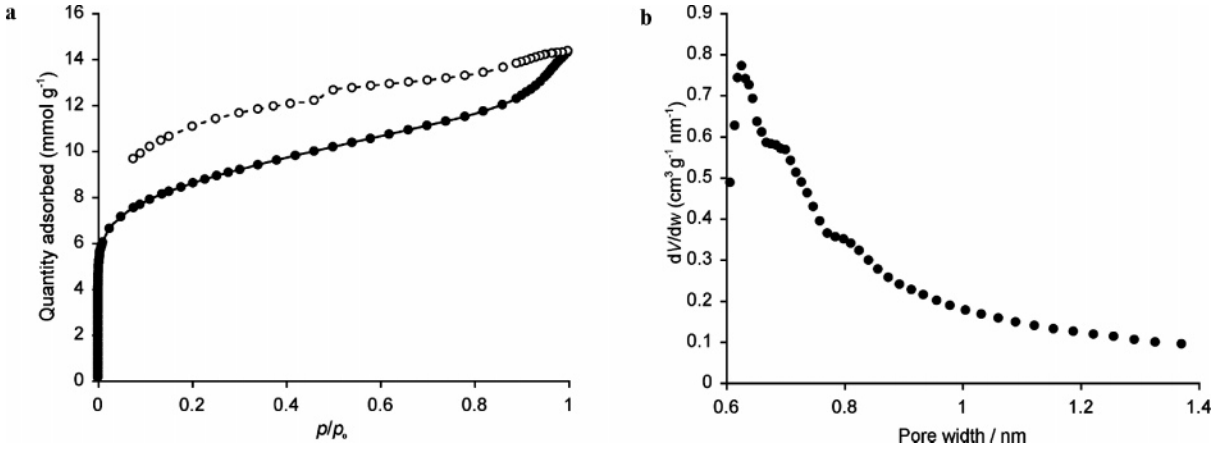

Figure 3. (a) The N_2 adsorption isotherm of a powdered sample of **PIM-7**. The adsorption data points are shown as ● and desorption points as ○. BET analysis gives an apparent surface area of 680 m^2 g^{-1}. (b) The pore size distribution derived from the low-pressure N_2 adsorption data using the Horvath−Kawazoe method.

Table 1. BET Surface Areas of PIMs-7−10 and Cardo-PIMs-1 and 2 Derived from N_2 Adsorption Isotherms

	PIM-7	PIM-8	PIM-9	PIM-10	Cardo-PIM-1	Cardo-PIM-2
surface area (m^2 g^{-1})	680	677	661	713	621	580
pore volume (cm^3 g^{-1})	0.56	0.48	0.47	0.44	0.51	0.63

analysis also indicates the presence of a low percentage of chlorine in these polymers (e.g., less than 0.3% for **PIM-7** derived from the optimized polymerization reactions). Matrix assisted laser desorption ionization mass spectrometry (MALDI-MS) analysis of the low-mass fraction obtained during the purification of polymers **PIMs-7−9** and **Cardo-PIM-1** suggests that a high proportion of the oligomeric products are cyclic structures (e.g., Figure 2), with a family of peaks representing the [2 + 2], [3 + 3], [4 + 4], and [5 + 5] cyclic oligomers. Kricheldorf has established that the dioxane-forming polymerization between fluorinated monomers and monomer **1** produces cyclic oligomers and contends, based on convincing data from MALDI-MS, that even high-molar mass macromolecules of polymers such as **PIM-1** are predominately cyclic.[37−39] We could not obtain MALDI MS data from higher molecular mass fractions to establish whether this is similar for **PIMs-7−9**. In contrast, MALDI-MS analysis of the low-molar mass fraction of **PIM-10** does not indicate the formation of a significant amount of cyclic oligomers. This may be related to the absence of spiro-centers within the structure of **PIM-10** that have been shown previously by molecular modeling to allow some flexibility within the polymer, which may assist the formation of cyclics.[40]

Nitrogen Adsorption. Nitrogen adsorption isotherms measured at 77 K confirms that **PIMs-7−10** are microporous (e.g., Figure 3) as shown by the significant adsorption at low pressure (P/P_o < 0.1). BET analysis of the isotherms provides an apparent surface area for each polymer of more than 650 m^2 g^{-1} (Table 1). Analysis of the low-pressure nitrogen adsorption data by the Horvath−Kawazoe method[41] indicates that the pore size distribution within **PIM-7** is strongly biased toward subnanometer pores. The nitrogen adsorption also shows that a thin solvent cast film of **PIM-7** (55 μm) displays an apparent high surface area of 507 m^2 g^{-1}. **Cardo-PIMs-1** and **2** also display microporosity but with slightly lower apparent surface areas (Table 1). In contrast the model compound **5** lacks significant surface area (<5 m^2 g^{-1}) demonstrating the need for a polymeric structure to obtain microporosity.

Thermal Stability. Thermal gravimetric analysis (TGA) showed a small mass loss (2−3%) for each polymer up to 200 °C which may be due to entrapped solvent or water. **PIM-7** starts to degrade only above 480 °C whereas **PIMs-8−10** and

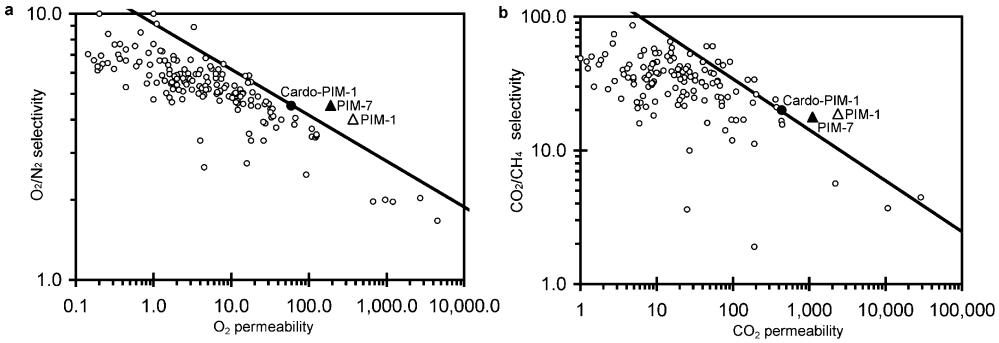

Figure 4. Robeson plots of permeability versus selectivity for the (a) O_2/N_2 and (b) CO_2/CH_4 gas pairs. The — represents the original upperbound[42] and the ○ represent data points for polymers reported since 1991.

Table 2. Gas Transport Properties for PIM-7 and Cardo-PIM-1

polymer	gas	P_x (Barrer)	D_x (10^{-8} cm^2 s^{-1})	S_x (10^{-3} cm^3 cm^{-3} cmHg^{-1})	P_x/P_{N_2}
PIM-7	O_2	190	62	31	4.5
PIM-7	N_2	42	16	26	1.0
PIM-7	He	440	900	5	10
PIM-7	Ar	100	30	33	2.4
PIM-7	Xe	26	0.37	700	0.62
PIM-7	H_2	860	1100	8	20
PIM-7	CO_2	1100	21	520	26
PIM-7	CH_4	62	5	120	1.5
Cardo-PIM-1	O_2	59	23	25	4.5
Cardo-PIM-1	N_2	13	6	21	1.0
Cardo-PIM-1	He	170	1200	1.6	13
Cardo-PIM-1	Ar	33	11	29	2.5
Cardo-PIM-1	H_2	320	680	5	25
Cardo-PIM-1	CO_2	430	8	560	33
Cardo-PIM-1	CH_4	22	2	110	1.7

Cardo-PIM-2 lose significant mass (4−6%) between 380 and 450 °C which may be associated with the loss of ethene from the bridged structural unit derived from monomer **2** via a retro-Diels−Alder reaction. In all cases, thermal degradation in nitrogen results in a loss of mass of only 20−30% up to 700 °C, indicating that carbonization is occurring.

Gas Permeability. The gas permeabilities (P_x) and ideal gas selectivities relative to N_2 (P_x/P_{N_2}) for the two good film-forming polymers **PIM-7** and **Cardo-PIM-1** are given in Table 2. For both polymers the values of P_x are relatively high and the order of permeability (P_x) is $CO_2 > H_2 > He > O_2 > Ar > CH_4 > N_2 > Xe$ which is unusual for glassy polymers for which $P_{He} > P_{CO_2}$ is typical. A desirable polymer-based gas separation membrane requires both high permeability and high selectivity; however, for polymer gas separation membranes there is a tradeoff between permeability and selectivity. This tradeoff was quantified by Robeson in 1991 who delineated an upper-bound on plots of log P_x versus log P_x/P_y for a number of gas pairs using an exhaustive list of existing permeability data.[42] With the notable exception of **PIM-1**,[20] most highly permeable polymers studied since 1991 (i.e., those with $P_{O_2} > 100$ Barrer) fall well below the upper-bound. However, the permeability data for **PIM-7** lies significantly above the Robeson upper-bound for most gas pairs including the commercially important O_2/N_2 (Figure 4a) and CO_2/CH_4 (Figure 4b) whereas the points for **Cardo-PIM-1** lies approximately on the upper-bound line for these two gas pairs. It was noted by Robeson that polymers which lay on the upper-bound were rigid-chain glassy polymers whereas rubbery polymers with flexible chains fell far below the upper-bound.[42] Freeman,[43] and later Cecopieri-Gómez and co-workers,[44] have developed a theory to rationalize this observation and justify an empirical principle which predicts that to obtain the best permeability/selectivity properties, one needs to create a polymer structure with a stiff backbone, which enhances mobility selectivity at the expense of diffusivity, while also disrupting interchain packing to improve permeability. PIMs follow this principle closely. The poorer performance of **Cardo-PIM-1** reflects the greater conformational freedom and flexibility of the polymer chain, which can be attributed to the fluorene-based cardo units. Another contributing factor to the excellent performance of PIMs is the remarkably high solubility coefficients for each gas (Table 1) which enhances permeability without diminishing selectivity.[20] The high apparent solubility of gases in PIMs may be attributed to the microporous character of PIMs, which provides a high capacity for gas uptake, as shown by the nitrogen adsorption measurements, coupled with chemical functionality that strengthens intermolecular interactions and encourages sorption. In particular, the polarizability of the predominately aromatic structure of **PIM-7** would enhance the van der Waals interactions between the polymer and gas.

Conclusions

The synthetic trick of converting a biscatechol monomer into a bis(phenazine)-based tetrahalide monomer suitable for making PIMs broadens considerably the potential diversity of this promising class of polymer. Tetrahalide monomers containing a "site of contortion" such as the spiro-center in monomer **4** allows the use of a greater number of biscatechol monomers, which would otherwise lead to linear polymers that pack efficiently in space to give a dense, nonmicroporous material. The promising gas permeability data for **PIM-7** confirms that the concept of PIMs is an excellent one for designing highly rigid but solution-processible polymers, which combine high selectivity with high permeability as required for the fabrication of efficient gas separation membranes.

Acknowledgment. We thank the EPSRC for funding.

References and Notes

(1) Davankov, V. A.; Tsyurupa, M. P. *React. Polym.* **1990**, *13*, 27.
(2) Tsyurupa, M. P.; Davankov, V. A. *React. Funct. Polym.* **2002**, *53*, 193.
(3) Webster, O. W.; Gentry, F. P.; Farlee, R. D.; Smart, B. E. *Makromol. Chem., Macromol. Symp.* **1992**, *54/55*, 477.
(4) Urban, C.; McCord, E. F.; Webster, O. W.; Abrams, L.; Long, H. W.; Gaede, H.; Tang, P.; Pines, A. *Chem. Mater.* **1995**, *7*, 1325.
(5) Wood, C. D.; Tan, B.; Trewin, A.; Niu, H. J.; Bradshaw, D.; Rosseinsky, M. J.; Khimyak, Y. Z.; Campbell, N. L.; Kirk, R.; Stockel, E.; Cooper, A. I. *Chem. Mater.* **2007**, *19*, 2034.
(6) Ghanem, B.; McKeown, N. B.; Harris, K. D. M.; Pan, Z.; Budd, P. M.; Butler, A.; Selbie, J.; Book, D.; Walton, A. *Chem. Commun.* **2007**, 67.
(7) McKeown, N. B.; Gahnem, B.; Msayib, K. J.; Budd, P. M.; Tattershall, C. E.; Mahmood, K.; Tan, S.; Book, D.; Langmi, H. W.; Walton, A. *Angew. Chem., Int. Ed.* **2006**, *45*, 1804.
(8) McKeown, N. B.; Hanif, S.; Msayib, K.; Tattershall, C. E.; Budd, P. M. *Chem. Commun.* **2002**, 2782.
(9) McKeown, N. B.; Makhseed, S.; Budd, P. M. *Chem. Commun.* **2002**, 2780.
(10) Budd, P. M.; Ghanem, B.; Msayib, K.; McKeown, N. B.; Tattershall, C. *J. Mater. Chem.* **2003**, *13*, 2721.
(11) Masuda, T.; Isobe, E.; Higashimura, T.; Takada, K. *J. Am. Chem. Soc.* **1983**, *7473*.
(12) Nagai, K.; Masuda, T.; Nakagawa, T.; Freeman, B. D.; Pinnau, I. *Prog. Polym. Sci.* **2001**, *26*, 721.
(13) Tanaka, K.; Okano, M.; Toshino, H.; Kita, H.; Okamoto, K. I. *J. Polym. Sci., Polym. Phys.* **1992**, *30*, 907.
(14) Yu, A.; Shantarovich, V.; Merkel, T. C.; Bondar, V. I.; Freeman, B. D.; Yampolskii, Y. *Macromolecules* **2002**, *35*, 9513.
(15) Budd, P. M.; Elabas, E. S.; Ghanem, B. S.; Makhseed, S.; McKeown, N. B.; Msayib, K. J.; Tattershall, C. E.; Wang, D. *Adv. Mater.* **2004**, *16*, 456.
(16) Budd, P. M.; Ghanem, B. S.; Makhseed, S.; McKeown, N. B.; Msayib, K. J.; Tattershall, C. E. *Chem. Commun.* **2004**, 230.
(17) Budd, P. M.; McKeown, N. B.; Fritsch, D. *J. Mater. Chem.* **2005**, *15*, 1977.
(18) McKeown, N. B.; Budd, P. M.; Msayib, K. J.; Ghanem, B. S.; Kingston, H. J.; Tattershall, C. E.; Makhseed, S.; Reynolds, K. J.; Fritsch, D. *Chem.—Eur. J.* **2005**, *11*, 2610.
(19) McKeown, N. B.; Budd, P. M. *Chem. Soc. Rev.* **2006**, *35*, 675.
(20) Budd, P. M.; Msayib, K. J.; Tattershall, C. E.; Ghanem, B. S.; Reynolds, K. J.; McKeown, N. B.; Fritsch, D. *J. Membr. Sci.* **2005**, *251*, 263.
(21) Budd, P. M.; Butler, A.; Selbie, J.; Mahmood, K.; McKeown, N. B.; Ghanem, B.; Msayib, K.; Book, D.; Walton, A. *Phys. Chem. Chem. Phys.* **2007**, *9*, 1802.
(22) McKeown, N. B.; Budd, P. M.; Book, D. *Macromol. Rapid Commun.* **2007**, *28*, 995.
(23) Maffei, A. V.; Budd, P. M.; McKeown, N. B. *Langmuir* **2006**, *22*, 4225.
(24) Niederl, J. P.; Nagel, R. H. *J. Am. Chem. Soc.* **1940**, *62*, 3070.
(25) Le Goff, E. *Angew. Chem.* **1962**, 490.
(26) Musgrave, O. C.; Davidson, I. M. *J. Chem. Soc.* **1963**, 3154.
(27) Apel, S.; Nitsche, S.; Beketov, K.; Seichter, W.; Seidel, J.; Weber, E. *J. Chem. Soc., Perkin Trans. 1* **2001**, 1212.
(28) Baker, D.; McGowan, J. C. *J. Chem. Soc.* **1943**, 486.
(29) Jacob, P.; Callery, P. S.; Shulgin, A. T.; Castagnoli, N. *J. Org. Chem.* **1976**, *41*, 3627.
(30) Engelmann, I.; Schultze, J. D.; Bohning, M.; Springer, J. *Makromol. Chem., Macromol. Symp.* **1991**, *50*, 79.
(31) Korikov, A. P.; Vygodskii, Y. S.; Yampol'skii, Y. P. *Polym. Sci., Ser. A* **2001**, *43*, 638.
(32) Kazama, S.; Teramoto, T.; Haraya, K. *J. Membr. Sci.* **2002**, *207*, 91.
(33) Wang, Z. G.; Chen, T. L.; Xu, J. P. *J. Appl. Polym. Sci.* **2002**, *83*, 791.
(34) Chen, C. H.; Shu, C. F. *J. Polym. Sci., Polym. Chem.* **2004**, *42*, 3314.
(35) Kazama, S.; Teramoto, T.; Haraya, K. *High Perform. Polym.* **2005**, *17*, 3.
(36) Camacho-Zuniga, C.; Ruiz-Trevino, F. A.; Zolotukhin, M. G.; del Castillo, L. F.; Guzman, J.; Chavez, J.; Torres, G.; Gileva, N. G.; Sedova, E. A. *J. Membr. Sci.* **2006**, *283*, 393.
(37) Kricheldorf, H. R.; Fritsch, D.; Vakhtangishvili, L.; Schwarz, G. *Macromol. Chem. Phys.* **2005**, *206*, 2239.
(38) Kricheldorf, H. R.; Fritsch, D.; Vakhtangishvili, L.; Lomadze, N.; Schwarz, G. *Macromolecules* **2006**, *39*, 4990.
(39) Kricheldorf, H. R.; Lomadze, N.; Fritsch, D.; Schwarz, G. *J. Polym. Sci., Polym. Chem.* **2006**, *44*, 5344.
(40) Heuchel, M.; Fritsch, D.; Budd, P. M.; McKeown, N. B.; Hofmann, D. Unpublished results, 2007.
(41) Horvath, G.; Kawazoe, K. *J. Chem. Eng. Jpn.* **1983**, *16*, 470.
(42) Robeson, L. M. *J. Membr. Sci.* **1991**, *62*, 165.
(43) Freeman, B. D. *Macromolecules* **1999**, *32*, 375.
(44) Cecopieri-Gomez, M. L.; Palacios-Alquisira, J.; Dominguez, J. M. *J. Membr. Sci.* **2007**, *293*, 53.

MA071846R